Highlights on Spanish Astrophysics X, Proceedings of the XIII Scientific Meeting of the Spanish Astronomical Society held on July 16 – 20, 2018, in Salamanca, Spain. B. Montesinos, A. Asensio Ramos, F. Buitrago, R. Schödel, E. Villaver, S. Pérez-Hoyos, I. Ordóñez-Etxeberria (eds.), 2019

The Hα Luminosity Function and the Star Formation Rate Density of the local Universe with J-PLUS DR1 data.

Gonzalo Vilella-Rojo[1], Rafael Logroño-García[1], Carlos López-Sanjuan[1], Jesús Varela[1], Kerttu Viironen[1], and The J-PLUS team

[1] Centro de Estudio de Física del Cosmos de Aragón, Unidad Asociada al CSIC, Plaza San Juan 1, 44001 Teruel, Spain

Abstract

The First Data release of the J-PLUS photometric survey is already public and available for the scientific community. It includes millions of sources in a usable area of 897 deg^2. With it, we analyse nearby star-forming galaxies ($z < 0.017$) to obtain the Hα Luminosity Function of the Local Universe, the Star Formation Main Sequence, and the Star Formation Rate Density of the Local Universe. Our results are the most local values for these properties, using a large and homogeneous sample of sources with no target pre-selection.

1 Introduction

The Javalambre Photometric Local Universe Survey (J-PLUS, hereafter) is a photometric survey conducted from the Observatorio Astrofísico de Javalambre, in Teruel, Spain. It is carried out using an 83 cm diameter telescope (JAST/T80) and a large camera (T80Cam) that provide an effective Field of View of 2 square degrees. The filter system includes a set of 5 broadband filters (almost identical to the SDSS photometric system), and 7 medium and narrow bands, placed in key stellar features. All the details of the J-PLUS survey can be found in [2].

In this contribution we present the first determination of the Hα Luminosity Function at $z = 0$ with the homogeneous sample of sources present in the first J-PLUS Data Release. In Section 1, we present the properties of the data sample. In Section 2, we describe the process to select sources with an emission line inside the J0660 filter. Section 3 summarizes the criteria to discern objects at low redshift from contaminants at higher redshift. The Luminosity Function, Star Formation Main Sequence, and Star Formation Rate Density are presented in Section 4. Finally, we discuss the results and summarize the main points of this

contribution in Section 5.

2 Data

In this Section we present the main characteristics of the J-PLUS first Data Release (DR1 hereafter). J-PLUS DR1 includes high-quality multiband information of 897 deg^2 (1022 deg^2 before masking), around 8.4 million objects with $r < 21$ detected in dual mode, including stars, galaxies, or QSO. Aside from the photometry, value-added catalogs are provided with extra information, that includes photometric redshifts, object classification, or cross-matches with pre-existing catalogs, among others. It is publicly accessible via ADQL queries in the J-PLUS website[1]. Custom queries can be performed to retrieve data according to different criteria. J-PLUS DR1 is described in these proceedings by López-Sanjuan *et al.*

For this study, we select all objects with $r \leq 18$. We apply this cut to ensure that we are complete in detection. We do not expect this to significantly bias our selection due to the nature of our sources. Star-forming galaxies in the nearby Universe should not be much fainter than this cut, and it helps to filter contaminants at higher redshift, which will be mainly [OIII] emitters at $z \sim 0.3$.

3 Emitter Selection

In this Section we explain the method that we use to select sources with an emission inside the J0660 filter, and how we discern between low-z and high-z emitters. We recall here that the [OIII] emission is within the J0660 wavelength range at $z \sim 0.3$.

To select emitters at low-z, we retrieve all $J0660$, r, and i fluxes from the database. We infer a linear continuum that spans from the central wavelength of r, to the central wavelength of i, thus inferring a local continuum for $J0660$ at the wavelength range of Hα. All the equations and details about this method can be found in Vilella-Rojo *et al.*, 2015 [12].

We do this in a Monte-Carlo approach. We perform many iterations of this routine, varying each time the value of the flux inside each filter within its error bar, assigning each time a component of noise that is drawn from a Gaussian distribution with σ that is the photometric error of each flux. Each time we do this, we store the obtained value. In the end, each source has a N values of excess inside $J0660$, where N is the number of iterations that we repeated this process. In the end we consider as emitters all sources that fulfill the condition

$$\frac{\langle F \rangle}{\mathrm{NMAD}\,(F)} \geq 3 \tag{1}$$

where $\langle F \rangle$ is the median of all the N excess measurements for each source, and NMAD (F) is the normalized median absolute deviation, as given by $1.48 \times \mathrm{median}\,(\,|\,F_i - \langle F \rangle\,|\,)$.

[1] http://www.j-plus.es/

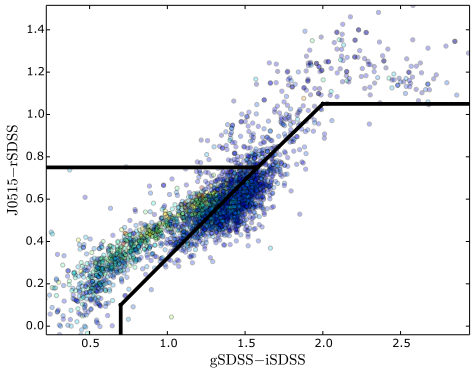

Figure 1: Color-color plot used to separate sources. Dots are color-coded according to the area of the `SExtractor` ellipse that encloses the source. Three regions are drawn according to the nature of the sources. The upper region is a stellar locus. Lower right region contains galaxies at a redshift higher than our redshift of interest. Low redshift galaxies are clustered in the lower left region.

All the emitting sources are then plotted in a $J0515 - r$ *vs* $g - i$ color-color diagram. In Figure 1 we plot this diagram. Dots are color coded according to the area of the ellipse of the detection in `SExtractor` MAG_AUTO mode using the r filter as the detection band.

We cross-match all the sources with preexisting catalogs that include spectroscopic redshifts. We find that low-z objects are populating a sequence in the lower left corner. Sources with a redshift higher than our redshift of interest are clustered around $g - i \sim 1.5$. We select all the sources that are candidates to be low redshift, and we check them by eye to classify them as low redshift emitters. The numbers that describe this sample are summarised in Table 1

Table 1: Summary of redshift distribution of the candidates that lie within the region of low-z candidates inside the color-color diagram.

With spec-z		Without spec-z		
Low z	High z	Low z candidates	High z candidates	Total
466	485	166	431	1548

The final sample of low z galaxies contains 632 galaxies. The purity of this sample should be around 100%; we might not be complete, but given the cuts that we apply in the color-color diagram, and the visual inspection, we do not expect completeness to significantly bias our results.

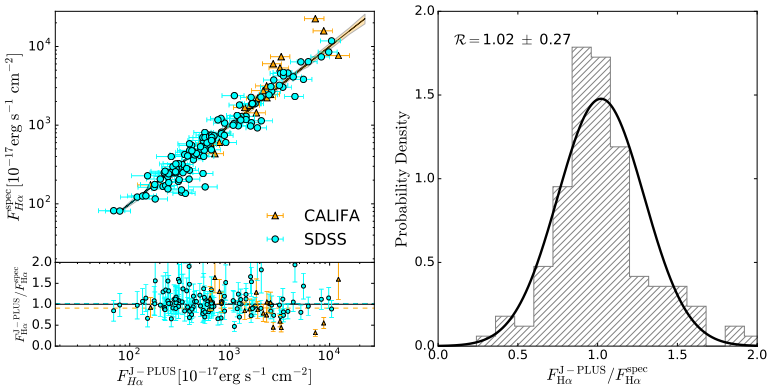

Figure 2: **Left panel:** Comparison between the clean Hα flux as measured with J-PLUS, and SDSS or CALIFA, for a sample of galaxies that are observed in the three surveys. **Right panel:** Histogram of the Ratio R between the Hα flux measured with J-PLUS and the spectroscopic values.

3.1 Performing the photometry

Once we identify our sources of interest, we repeat the photometry using only the emitting regions of each galaxy. This routine is described in detail in the work by Logroño-García *et al.* [6]. With it, we retrieve the photometry in the 12 J-PLUS filters, and with these we measure the Hα+[NII] excess. The Hα flux is then obtained using the SED-fitting method and corrections described in Vilella-Rojo *et al.*, 2015 [12]. The reliability of this method is tested against spectroscopic data, using galaxies in common with the SDSS and CALIFA surveys. Results can be found in [6] and in Figure 2 in this contribution.

4 Results

In this Section we present the main results of this study. These include the Hα Luminosity Function (Hα LF), the Galaxy Star Formation Main Sequence, and the Star Formation Rate Density ρ_* in the local volume.

4.1 The Hα Luminosity Function

To compute the distance to our galaxies, we use the spectroscopic redshift when these are available. Sources without spectroscopic redshift are assigned a random distance according to a volume prior. We do this with all the sources 5000 times. Each round we assign a different distance, hence a different luminosity. In each iteration, we stack the resulting luminosities, and in the end we normalize the number counts.

To correct for completeness in volume, we apply the classical V/V_{max} technique described in Schmidt, 1968 [11]. Errors are estimated assuming a Poissonian distribution for

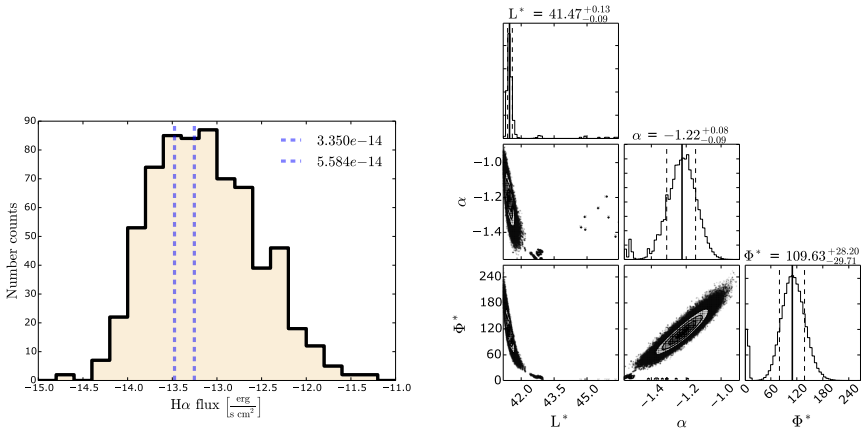

Figure 3: **Left panel:** Histogram of the Hα fluxes, and the flux cuts that we apply. **Right panel:** Probability distribution for each parameter of the fitting. Values in the titles represent the median, while errors correspond to the 16^{th} and 84^{th} percentiles of the stacked distributions.

the number counts. Finally, we fit the resulting distribution of number counts to a Schechter 1976 function:

$$n\left(L\right)\mathrm{d}L = \phi^{*}\left(\frac{L}{L^{*}}\right)^{\alpha} e^{\frac{L}{L^{*}}}\frac{\mathrm{d}L}{\mathrm{d}L^{*}}. \tag{2}$$

To perform the fitting and explore the parameter space, we use a MCMC approach. We use the code `emcee` [3]. We sample the 3-dimensional parameter space (i.e. L^{*}, α, and ϕ^{*}) for different 11 different values of limiting flux equally spaced between 3.35×10^{-14} and $5.58 \times 10^{-14}\,\mathrm{erg\,s^{-1}}$. These cuts can be found in Figure 3. We do this to include the uncertainty in the emission-line completeness in the final error of our parameters. We stack all the sampler chains and perform the statistical analysis in the resulting stacking. This is shown in Figure 4.

For each of the 11 values of limiting flux, we perform a fitting to a Schechter distribution (see [10]). We present the individual LFs, and the average one, in Figure 4

The values that we obtain for the fitting are: $\log_{10}\left(L^{*}\right) = 41.47\,\pm^{0.13}_{0.09}\,\left[\frac{\mathrm{erg}}{\mathrm{s}}\right]$, $\alpha = -1.22\pm^{0.08}_{0.09}$, $\log_{10}\left(\phi^{*}\right) = -2.55\,\pm^{0.1}_{0.13}\,\left[\mathrm{Mpc}^{-3}\right]$.

The integral of this distribution is analytical under the condition $\alpha \leq -2$,

$$\mathcal{L} = \int \phi^{*}\frac{L}{L^{*}}\exp\left(-\frac{L}{L^{*}}\right)\frac{\mathrm{dL}}{L^{*}} = \phi^{*}L^{*}\Gamma\left(\alpha+2\right). \tag{3}$$

4.2 The Star Formation Rate Density at $z = 0$

To estimate the Star Formation Rate Density ρ_{*} of the local volume (up to ~ 73 Mpc distance in radius) we use the the Kennicutt (1998) relation (see [5]). This relation assumes a Salpeter [9] Initial Mass Function, and case B recombination.

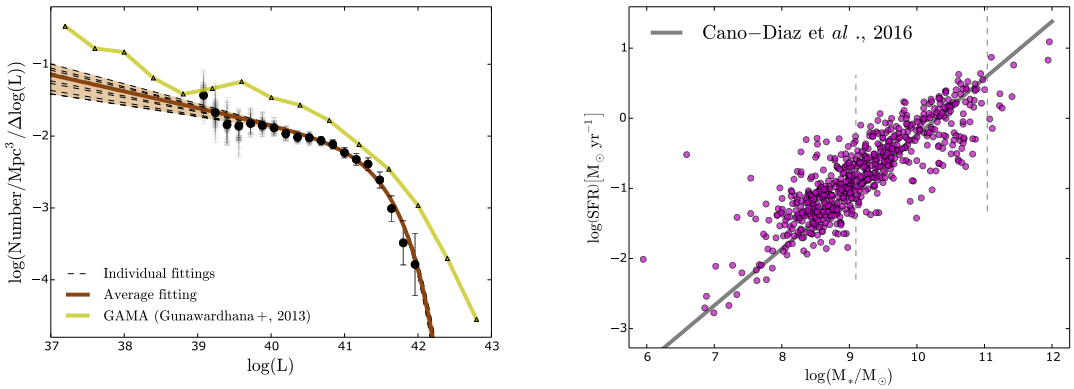

Figure 4: **Left panel**: Hα Luminosity Function. Grey dots represent the frequencies for each of the 11 realizations with different limiting flux. Black dashed lines are the individual fittings that are obtained with each limiting flux cut. Solid brown curve is the curve that has the median values for each of the three parameters. **Right panel:** Galaxy Star Formation Main Sequence obtained with J-PLUS DR1 data. Dashed vertical lines are 5$^{\text{th}}$ and 95$^{\text{th}}$ percentiles of the masses in the Cano-Díaz *et al.*, 2016, CALIFA sample

$$\text{SFR} = 7.9 \times 10^{-42} \mathcal{L} \quad \frac{\text{M}_\odot}{\text{year}}, \tag{4}$$

where $\mathcal{L}$ is the total luminosity of Hα, as computed from Equation 3. If we divide by the total volume up to $z = 0.017$, we obtain a SFRD $\log(\rho_*) = -2.10 \pm^{0.04}_{0.05}$. This is in good agreement with previous values in the literature (see, for instance [4]).

4.3 The Galaxy Star Formation Main Sequence

Finally, we plot the so called as Galaxy Star Formation Main Sequence [8], which relates the SFR of galaxies with their total stellar mass, M$_*$. This is shown in Figure 4. We overplot the fitting for the relation M$_*$ (SFR) obtained with spectroscopic data from the CALIFA Survey, as found in Cano-Díaz *et al.*, 2016.[1]. We find an excellent agreement between our measurements and CALIFA ones, giving us strong confidence in our findings.

5 Summary and conclusions

In this work we have presented three main results that are derived from the J-PLUS first Data Release, publicly available to the community in the J-PLUS website. These are the Hα Luminosity Function, the Star Formation Rate Density of the local Universe, and the Galaxy Main Sequence of Star Formation of a sample of 632 Hα emitters. To do that, we first selected all our sources from the catalogs, and to make sure that our sample was pure, we visually checked more than 1500 candidates.

After this visual inspection, our sample of emitters includes 632 galaxies, of which 166 had not been previously assigned a redshift. These galaxies present compact morphologies and blue colors, being an interesting population for further analysis.

The Hα LF shows consistency with previous values in the literature. It is in good agreement with a Schechter distribution, which allows us to perform an analytical integral to compute the total Hα luminosity and the star formation rate density. This value is also in agreement with previous studies.

Finally, we compute the Galaxy Star Formation Main Sequence, which relates the star formation rate of a galaxy with its mass, and shows a correlation that spans for 3 orders of magnitude. We compare our result with the one obtained using spectroscopic measurements from the CALIFA survey, showing not only an excellent agreement, but a wider mass range.

References

[1] Cano-Díaz, M., et al., 2016, ApJ, 821, 26

[2] Cenarro, A.J., et al. 2018, A&A submitted, arXiv:1804.02667

[3] Foreman-Mackey, D., et al., 2013, PASP, 125, 306

[4] Gunawardhana et al., 2013, 433, 2764

[5] Kennicutt, R. C. 1998, ARA&A, 36, 189

[6] Logroño-García, R. et al. 2018, A&A accepted, arXiv:1804.04039

[7] López-Sanjuan, C., et al. 2018, A&A accepted, arXiv:1804.02673

[8] Noeske, K., et al., 2007, ApJ, 660, 43

[9] Salpeter, EE. 1955, ApJ, 121, 161

[10] Schechter, P. 1976, ApJ, 203, 297

[11] Schmidt, M. 1968, ApJ, 151

[12] Vilella-Rojo, G. et al. 2015, A&A, 580, A47